

The Flame Temperature of the Laminar Premixed Flame with Spatially Changing Stretch Rate along the Flame Surface

Takeshi Yokomori* and Masahiko Mizomoto**

* School of Science for Open and Environmental Systems, Graduate School of Keio University

**Department of Mechanical Engineering, Keio University

3-14-1 Hiyoshi, Kouhoku-ku Yokohama, Kanagawa, 223-8522, JAPAN

E-mail: y10442@educ.cc.keio.ac.jp

Keywords : Laminar Premixed Flame, Flame Temperature, Flame Stretch, Preferential Diffusion, Lewis Number

Introduction

The flame stretch concept provides us with great understanding of the phenomena of premixed combustion. Especially, the flame stretch concept may be useful for understanding the structure of a wrinkled laminar premixed flame in a turbulent flow or a thermal-diffusive unstable flame. In many past studies, however, such concept was discussed in the case that the effects of flame stretch and preferential diffusion are assumed not to change along the flame surface. Therefore, traditional theoretical predictions will not accurately estimate the changes in the burning intensities of a wrinkled laminar flame or a thermal-diffusive unstable flame, since adjacent flame segments with different burning intensities may interact with each other and thus vary the burning intensities.

In the present study, we investigated the variation in the flame temperature, which has the spatially non-uniform stretch rate along the flame surface. We made a multiple-slit burner to stabilize the corrugated laminar premixed flame. The flame temperature and the flame stretch rate (designating both flame curvature and flow field strain) were measured, and then we examined the relationship between them theoretically.

Experimental Procedure

The essential feature of the burner and the orientation of the coordinates used in the present study are shown in Fig. 1. Three thin plates, each 0.3 mm thick, were placed on the burner so as to divide a rectangular channel into four equal slits of 4.0 mm \times 35.0 mm cross-section. This burner allowed a corrugated stable flame (3V-type) or a Inverted flame (V-type) to form. Lean propane/air premixed mixtures were provided, and the Lewis numbers were greater than unity.

To estimate the stretch rate, we adopted the laser tomographic visualization technique to measure the flame front shape, and particle image velocimetry (PIV) to measure the velocity distribution. The detailed features of the burner and measurement techniques are addressed in Ref.1

The temperature was measured by a thermocouple, which

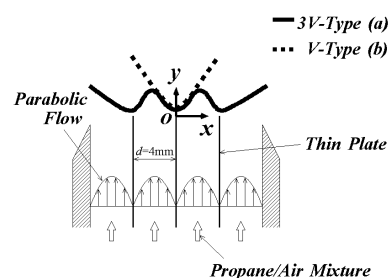


Fig.1 Schematic of the burner

consisted of Pt80%/Rh20%- Pt60%/Rh40% with 100 mm diameter wires. The wires were coated in silica to prevent catalytic heating on the surface, and our temperature measurements corrected for radiative heat loss.

Result and Discussion

For the 3V-types, the average velocity of the mixture was set near the blowoff limit in order to minimize the heat loss from the flame to the thin plate. For the V-types, the convex flame segment was stabilized at the mean velocity where the curvature of the convex was equal to that of the center convex of the 3V-type in each equivalence ratio. The equivalence ratios and the mean velocities used in this investigation are shown in Table1.

Equivalence ratio ϕ	Flame type	Average velocity (m/s)	Le
0.76	3V	0.77	1.73
0.76	V	0.91	1.73
0.72	3V	0.32	1.74
0.72	V	0.43	1.74
0.68	3V	0.24	1.75
0.68	V	0.30	1.75

Figure 2 shows the typical temperature distribution measured using the thermocouple on the burned gas side. For each equivalence ratio we extracted the flame temperature T_b from the burned gas temperature distribution like Fig.2 (the procedure is described in Ref.2, 3), the results are shown in Fig.3. The flame temperature is made dimensionless $\theta = (T_b - T_u) / (T_{ad} - T_u)$ using the unburned gas temperature T_u (298K), and the adiabatic temperature T_{ad} is estimated from the equilibrium calculation. On the other hand, The circle plots in Fig 4 show temperature profiles estimated from the stretch rate, using the following expression proposed by Sun et al[4]:

$$\theta = \frac{T_b - T_u}{T_{ad} - T_u} = 1 + \alpha^0 \tilde{\kappa} \left(\frac{1}{Le} - 1 \right) \quad (1)$$

where $\alpha^0 = \int_0^{\delta_r^0} (\rho / \rho_u) d\eta = 1 + \ln[T_u / T_{ad} + (1 - T_u / T_{ad}) e^{-1}]$, $\tilde{\kappa} = (\delta_r^0 / S_u^0) \kappa$, κ is the flame stretch rate, δ_r^0 is the flame thickness[4], and S_u^0 is the laminar burning velocity[5]. κ were measured using the laser tomographic visualization technique and PIV[2,3]. Here, in order to compare this estimated flame temperature with the measured one (Fig.3), the position of x was corrected by moving it from the flame front where κ was obtained to the burned side boundary where the flame temperature was measured by the

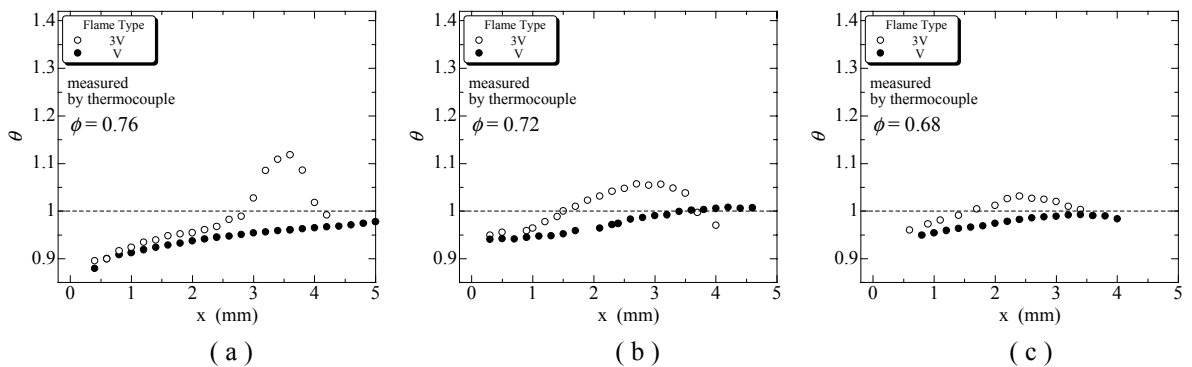


Fig.3 Nondimensional flame temperature measured by thermocouple along flame surface

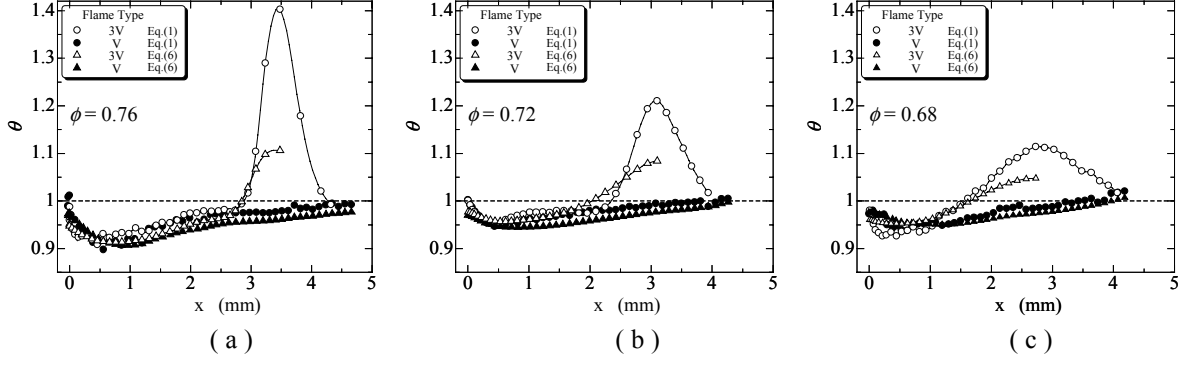


Fig.4 Nondimensional flame temperature estimated using Eq.(1) and Eq.(6)

thermocouple. Comparing Fig. 3 with Fig. 4, it seems that the tendencies of the 3V-type flames do not agree with the estimates, while those of the V-types agree well. In the 3V-type, especially, it is notable that the estimated flame temperature is much higher at the concave tip and is smaller at the neighbor of the concave (ex. for $\phi=0.72$, $x=1.5\sim 2.5\text{mm}$) than the measured temperature. The reason why these differences appear is that the heat transfer along the flame surface and to the burned gas is not considered in Eq.(1), although the temperature gradients exist in such directions as shown in Fig. 2.

Therefore, we take those conductive heat transfer effects into consideration by remodeling the theory of Sun et al [4], which is derived in the case of a uniform stretch rate along a flame surface. The flame and flow configuration is shown in Fig. 5. The thin reaction zone has an area A_f . The surface of the upstream boundary of the preheat zone at the distance δ_r from the reaction zone is intercepted by the streamtube, which corresponds to A_f ,

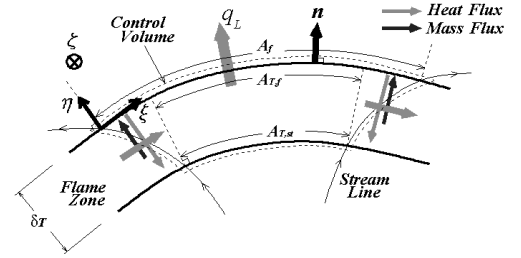


Fig.5 Schematic diagram of control volume composed of curved flame zone and nonuniform flow.

thus defining the area of streamtube $A_{T,st}$. Projecting $A_{T,st}$ onto the reaction zone surface yields $A_{T,f}$, which differs from $A_{T,st}$ because of the flame curvature. Moreover, a curvilinear orthogonal system of coordinates is introduced, in which the η axis is perpendicular to the flame surface, ξ and ζ are parallel with the flame surface, and ζ is at a right angle to ξ . If we assume that the flame is stationary and if we take the control volume as shown in Fig.5, the mass, the energy and the species conservation are as follows.

$$\rho_{u,T} U_{u,T} A_{T,st} = \rho_{u,M} U_{u,M} A_{M,st} = \rho_b U_b A_f \quad (2)$$

$$\begin{aligned} (\rho_b U_b A_f c_p T_b - \rho_{u,T} U_{u,T} A_{T,st} c_p T_u) + \lambda(A_f - A_{T,f}) \frac{(T_b - T_u)}{\delta_r} \\ - \lambda \frac{\partial}{\partial \xi} \left(d\zeta \int_0^{\delta_r} \frac{\partial T}{\partial \xi} d\eta \right) d\xi - \lambda \frac{\partial}{\partial \zeta} \left(d\xi \int_0^{\delta_r} \frac{\partial T}{\partial \zeta} d\eta \right) d\zeta = A_f q \langle Yk \rangle - q_L \end{aligned} \quad (3)$$

$$\rho_{u,M} U_{u,M} A_{M,st} Y_u + \rho D (A_f - A_{M,f}) \left(\frac{Y_u}{\delta_M} \right) = A_f \langle Yk \rangle \quad (4)$$

where T : temperature, Y : concentration of the reactant, U : the flow velocity, c_p : specific heat, ρ : density, λ : thermal conductivity, D : mass diffusivity, q : heat release rate, $\langle Yk \rangle = \int_{\eta_b^-}^{\eta_b^+} Yk \, d\eta = \rho D (dY/d\eta)|_{\eta_b^-}$, Yk : reaction rate, q_L : heat loss. Subscript T or M designates the upstream boundaries of the heat or mass diffusion zone, respectively, and subscript u or b designates the unburned or burned state, respectively. In the energy conservation, the conductive heat transfer along the flame surface is taken into consideration. The areas constituting the control volume have the following relations:

$$A_f - A_{T,f} = \alpha^0 (\delta_T / S_u^0) \kappa A_f \quad , \quad A_f - A_{M,f} = \alpha^0 (\delta_M / S_u^0) \kappa A_f \quad , \quad A_f = d\xi \, d\zeta \quad (5)$$

Approximating that the temperature profile is linear across the flame zone, it is described as $T = (T_b - T_u)(\eta / \delta_T) + T_u$. The definition of the adiabatic temperature is given by $c_p(T_{ad} - T_u) = qY_u$. Substituting Eq.(4) into Eq.(3) and applying the relations mentioned above, we obtain the flame temperature for the stretched flame,

$$\frac{1}{2} \delta_T \delta_T^0 \nabla_i^2 \theta - (1 + \alpha^0 \tilde{\kappa}) \theta + 1 + \alpha^0 \tilde{\kappa} \frac{1}{Le} - Q = 0 \quad Q = \frac{q_L}{\rho_u S_u^0 c_p (T_{ad} - T_u)} \quad (6)$$

where ∇_i^2 is the tangential second-order differential operator of the flame surface. δ_T is the stretched flame thickness ($\delta_T / \delta_T^0 = (k_b^0 / k_b)^{1/2} = \exp(Ze(1-\theta)/2)$, Ze is Zeldovich number). In this investigation it is considered that the heat conducts from the flame to the downstream (burned side), it is taken into account as the heat loss term ($q_L = q_{dw} = -\lambda_{dw}(dT/d\eta)$). Since Eq.(6) is the nonlinear differential equation on θ , we tried to obtain the solution using the tridiagonal matrix algorithm. For the boundary conditions, $d\theta/d\xi = 0$ at both the convex and the concave tip in the 3V-type. In the V-type, on the other hand, $d\theta/d\xi = 0$ at the convex tip, while $d^2\theta/d\xi^2 = 0$ at $x=4.2\text{mm}$. The results are shown as the triangle plots in Fig.4.

We can see that the temperatures estimated using Eq.(6) agree well with the measured temperature. Particularly, these temperatures at the concave tips of the 3V-type are much lower than the temperatures estimated using Eq.(1). In concave segments the gradients of the stretch rate change dramatically, so that the gradient of the flame temperature changes spatially as a result of the flame stretch and the preferential diffusion. Hence, the heat conducts out around the concave, and the heat transfers which we noticed have a large effect on the flame temperature. In addition, the estimated flame temperature with such heat transfers at the segment neighboring the concave tip is higher than that without heat transfers, and the former agrees more with the measured temperature than the latter does. This is attributed to the heat received from the concave. Therefore, the feature of Fig.4 verifies the importance of such heat transfers.

References

1. T. Yokomori, M. Mizomoto, *Proc. of the Combustion Institute*, vol.29, 2002 (in press)
2. T. Yokomori, M. Mizomoto, 18th ICDERS, Paper No.149, 2001
3. T. Yokomori, M. Mizomoto, *Transactions of JSME*, B67-664, p.3139, 2001 (in Japanese)
4. C. J. Sun, C. J. Sung, L. He, C.K. Law, *Combust. Flame*, vol.118(1/2), p.108, 1999
5. C.M. Vagelopoulos, F.N. Egolfopoulos, C.K. Law, *Proc. of the Combustion Institute*, vol.25, 1994, p.1341